International Journal of Pharmaceutics, 89 (1993) 91–102

IJP 02885

The organ targetability of small and large albumin microspheres containing free and HSA conjugated methotrexate

Chong-Kook Kim, Sung-Joo Hwang [1] and Myung Gull Lee

College of Pharmacy, Seoul National University, San 56-1, Shinlim-Dong, Kwanak-Gu, Seoul 151-742 (South Korea)

(Received 30 July 1991)
(Modified version received 9 March 1992)
(Accepted 21 April 1992)

Key words: Hydrophilic albumin microspheres; Small microspheres; Large microspheres; Methotrexate; Methotrexate-human serum albumin conjugate; Lung targeting; Liver targeting

Summary

The organ-targeting ability of [^{3}H]methotrexate ([^{3}H]MTX), [^{3}H]MTX-human serum albumin (HSA) conjugates, and small (mean volume diameter, 10.0 μm) and large (mean volume diameter, 22.4 μm) size hydrophilic albumin microspheres (HAMs) containing different ratios of [^{3}H]MTX-HSA conjugates to [^{3}H]MTX was evaluated after i.v. administration of the compounds, equivalent to 150 nCi via the tail vein of mice. The total radioactivity in the lung increased immediately in a few minutes after i.v. injection of the both small and large HAMs, and then declined for up to 3–4 weeks, apparently reaching a plateau thereafter. However, the radioactivity in the liver, spleen and kidney increased slowly during the rapid decrease in radioactivity in the lung. This suggested that the small and large HAMs administered could be entrapped rapidly in the lung through mechanical filtration because of their large size and slowly redistributed to the liver, spleen and kidney due to either the HAMs being degraded enough for the size to allow passage through the capillary beds of the lung and/or the release of [^{3}H]MTX or [^{3}H]MTX-HSA conjugates from the HAMs. The highest value of AUQ was obtained for the liver and lung from small (including [^{3}H]MTX-HSA conjugates) and large HAMs, respectively, and suggested that the small (including [^{3}H]MTX-HSA conjugates) and large HAMs have a better targeting ability to the liver and lung, respectively, than that of MTX or MTX-HSA conjugates. This is consistent with the higher value of r_e^* for the liver and lung from the small and large HAMs, respectively. Greater selectivity for the liver and lung from the small and large HAMs, respectively, is indicated by a t_e^* value greater than unity. The greater targeting efficiency of the small and large HAMs for the liver and lung is indicated by higher values of T_e^*. However, the liver targeting efficiency of the small HAMs appeared to be similar to that of [^{3}H]MTX-HSA conjugates.

Correspondence to: C.-K. Kim, College of Pharmacy, Seoul National University, San 56-1, Shinlim-Dong, Kwanak-Gu, Seoul 151-742, South Korea.

[1] *Present address:* College of Pharmacy, Chungnam National University, 220, Kung-Dong, Yousung-Gu, Daejeon 305-764, South Korea.

Introduction

One of the major challenges in the fields of cancer chemotherapy is to deliver the chemotherapeutic agents to the targeting sites at the proper

rates and in appropriate amounts. For this purpose, many attempts have been focussed on the development of drug delivery systems; liposomes (Kim and Park, 1987) and anticancer drug macromolecules, such as human serum albumin (HSA) and polypeptide conjugates (Halbert et al., 1987; Kim et al., 1989a). Albumin microspheres have also been proposed as a drug delivery system for the targeting of anticancer drugs to various organs and tissues (Kramer, 1976), and for sustained release of the drug at the targeted site (Yang, 1986; Willmot et al., 1989).

Methotrexate (MTX)-bovine serum albumin (BSA) conjugates were reported to increase the survival time of mice bearing the ascitic form of L1210 (Jacobs et al., 1971), and the conjugates were proven to be more effective than free MTX against subcutaneously transplanted Lewis lung carcinoma (Chu and Whiteley, 1979). Moreover, radioactive albumin is found to be absorbed into neoplastic cells (Bushi et al., 1961), and albumin is actively taken up into tumor cells by pinocytosis (Ryser, 1963). It was reported that over 30% of the total exchangeable albumin might be in the extravascular space, such as in the muscle and skin (Jusko and Gretch, 1976), and serum albumin has been demonstrated to accumulate at tumor sites (Cerrottini and Isliker, 1967). Some MTX-rabbit serum albumin (RSA) conjugates appeared to be taken up into tissues, and MTX was released slowly from the conjugates after intravenous (i.v.) administration of the conjugates to rabbits (Yoon et al., 1991). Therefore, hydrophilic albumin microspheres (HAMs) entrapping different ratios of MTX-HSA conjugates to MTX might constitute an effective drug delivery system for the chemotherapeutic agent.

The factors affecting passive targeting efficiency such as the localization and distribution of particles in the body are the route of administration, particle size, and particle surface characteristics (Torrado et al., 1989). It was reported (Burger et al., 1985) that i.v. delivery of particles larger than 7–12 μm leads to their mechanical filtration by the lung, whereas those between 3 and 12 μm will become entrapped within the capillary networks of the lung, liver and spleen. We were therefore prompted to prepare relatively small (mean volume diameter, 8.35–11.2 μm) and large (mean volume diameter, 13.0–30.6 μm) size HAMs and to evaluate their organ targeting ability.

In this paper, small and large size HAMs containing different ratios of [^{3}H]MTX-HSA conjugates to free [^{3}H]MTX were prepared and their organ-targeting ability was evaluated after i.v. injection of the HAMs via the tail vein of mice.

Materials and Methods

Materials

MTX was kindly supplied by Choong-Wae Pharmaceutical Co. (Seoul, Korea), and [3′,5′,7-^{3}H]MTX ([^{3}H]MTX, 250 mCi/mmol, TRA224) was purchased from Amersham International (Buckinghamshire, U.K.). HSA (fraction V) and 1-ethyl-3-(3-dimethylaminopropyl) carbodiimide hydrochloride (EDC, protein sequencing reagents) were products of Sigma Chemical Co. (St. Louis, MO). Sephadex® G-75-40 (particle size, 10–40 μm) was obtained from Pharmacia Fine Chemicals (Uppsala, Sweden) and semipermeable membrane (Spectra/Por®; Mol. wt. cut off, 6000–8000; cylinder diameter, 14.6 mm) was purchased from Spectrum Medical Ind. (Terminal Annex, Los Angeles, CA). Soluene-350® (0.5 N quaternary ammonium hydroxide in toluene) and Scinti-A® XF scintillation cocktail were products of Packard Instrument Co. (A Canberra Co., Downers Grove, IL). PPO/POPOP scintillation cocktail was prepared by dissolving 5.5 g of 2,5-diphenyloxazole (PPO, Sigma Chemical Co.) and 0.1 g of 1,4-[2-(5-phenyloxazolyl)]benzene (POPOP, Sigma Chemical Co.) in a mixture of 667 ml of toluene and 333 ml of Triton® X-100 (Duksan Pharmaceutical Co., Seoul, Korea). All other chemicals were reagent grade and used without further purification.

Synthesis of HSA-conjugated [^{3}H]MTX

Covalently bound [^{3}H]MTX-HSA conjugates were prepared by a slight modification of the reported method (Chu and Whiteley, 1977; Kim and Oh, 1988). Briefly, after the addition of MTX (30 mg, 120 μCi, dissolved in 3 ml of 0.01 N

NaOH) to HSA (150 mg, dissolved in 10 ml of distilled water), EDC (150 mg, dissolved in 3 ml of 0.05 N HCl) was added slowly to the above solution at pH 5.0–6.0 for 7 h. The reaction mixture was kept at 4°C overnight. The resultant solution was loaded on a Sephadex G-75-40 column (2.5 × 30 cm). The first conjugate fraction (dimers or polymers) was discarded and the remaining macromolecular fractions were pooled. Before lyophilization, the macromolecular fraction was dialyzed using a semipermeable membrane (Spectra/Por®) to remove buffer components and other small molecules such as [^{3}H]MTX. The ratios of [^{3}H]MTX to HSA in the conjugates were calculated according to the method described previously (Kim and Oh, 1988). The molar ratio of MTX to HSA in the conjugates was 17.6, and a similar value, 15.3, was also reported by Halbert et al. (1987) for the addition of 25.0 mg of EDC immediately to a mixture of 100 mg of BSA and 40 mg of MTX.

Preparation of small and large HAMs containing free and HSA-conjugated [^{3}H]MTX

Large HAMs were prepared following our previous chemical cross-linking and surface modification technique (Kim and Oh, 1988). Briefly, 1 ml of HSA solution containing free and/or conjugated MTX (equivalent to 4 mg of MTX, 16 μCi of [^{3}H] radioactivity and 100 mg of HSA) was dispersed in 20 ml of cotton seed oil. The resultant emulsion was diluted to 50 ml with cotton seed oil and homogenized at 1700 rpm for 20 min. This emulsion was placed in an ice bath and further emulsified using an ultrasonicator (Branson Cleaning Equipment Co., CN). Then, 2 ml of 25% glutaraldehyde solution as a cross-linker was added to the fine emulsion. After 1 h, 1.5 ml of glycine solution (200 mg/ml) was added and stirred for 1 h. The products were washed with anhydrous diethyl ether and then distilled water. The small HAMs were prepared by a slight modification of the above method for large HAMs. In brief, cotton seed oil containing 0.5% Span 80 was used instead of pure cotton seed oil. In addition, the small HAMs obtained were washed with anhydrous diethyl ether, suspended in absolute ethanol in an ice bath for 3 min with the aid of an ultrasonicator and washed with distilled water. Four types of small and large HAMs, respectively, were prepared having different ratios of [^{3}H]MTX-HSA conjugates to free [^{3}H]MTX; 1:0 (SHAMC and LHAMC), 3:1 (SHAMC3F and LHAMC3F), 1:1 (SHAMCF and LHAMCF) and 0:1 (SHAMF and LHAMF). Total amounts of [^{3}H]MTX and/or [^{3}H]MTX-HSA conjugates used in the preparation of the HAMs were equivalent to 16 μCi of ^{3}H radioactivity (equivalent to 4 mg of MTX) per 100 mg of HSA. The hydrophilicity of the HAMs prepared by the surface modification technique was evaluated by our laboratory (Kim and Oh, 1988) using the capillary rise technique (Longo and Goldberg, 1985).

Measurement of radioactivity entrapped in the small and large HAMs

The radioactivity (as expressed in terms of [^{3}H]MTX) entrapped in the small and large HAMs was determined using a liquid scintillation counter (Rack Beta, LKB-Wallac Co., Turku, Finland) as follows: an accurately weighed amount (2 mg) of each HAM was transferred to 20 ml of a scintillation vial, 1 ml of Soluene-350® was added, and the mixture was stored overnight at 50°C to dissolve the microspheres. After neutralizing the mixture with 5 N HCl, 10 ml of PPO/POPOP scintillation cocktail was added, and equilibrated in the dark at 25°C for 2 days to reduce color quenching.

Particle size analysis of the small and large HAMs containing free and / or HSA conjugated [^{3}H]MTX

Particle size of the small and large HAMs, which are suspended in 0.9% NaCl solution (Isoton® II, Coulter Electronics Ltd, Luton, U.K.), was measured using a Coulter Multisizer® (Coulter Electronics Ltd) with a 70 or 140 μm aperture. The mean diameter was determined from the particle size distribution of each HAM on a number or volume basis. The size distribution (polydispersity) was measured in terms of a SPAN factor expressed as:

$$\text{SPAN} = \frac{D_{90\%} - D_{50\%}}{D_{50\%}}$$

where $D_{90\%}$, $D_{50\%}$ and $D_{10\%}$ are the diameters where the given percentage of particles is smaller than that size (Torrado et al., 1989).

Animals

Male ICR mice, weighing 18–22 g, were purchased from the Laboratory Animal Center, Seoul National University (Seoul, Korea). The animals were fed commercial rodent chow (Samyang Co., Seoul, Korea) and tap water ad libitum.

Intravenous injection

The same total radioactivity, 150 nCi (dissolved or suspended in 0.2 ml of normal saline solution) of [^{3}H]MTX (treatment I), [^{3}H]MTX-HSA conjugates (treatment II) and four types of small HAMs: SHAMC (treatment III), SHAMC3F (treatment IV), SHAMCF (treatment V), and SHAMF (treatment VI), and four types of large HAMs: LHAMC (treatment VII), LHAMC3F (treatment VIII), LHAMCF (treatment IX), and LHAMF (treatment X) was injected via the tail vein of mice in 10–20 s. At each designated time point, four mice were killed by cervical dislocation, and the lung, liver, spleen, and kidney were removed, rinsed with cold normal saline, blotted dry with paper towel, and weighed. For the small HAMs, blood was also collected directly via heart puncture into a heparinized tube and was centrifuged immediately to reduce the possible 'blood storage effect' on the determination of total plasma radioactivity (Lee et al., 1984, 1986). A portion of each organ or plasma was solubilized with Soluene®-350, 1 ml/0.2 g of organ in a counting vial. The vial was kept at 50°C for 12 h, and 0.2 ml of isopropyl alcohol and 0.4 ml of 30% hydrogen peroxide were added to minimize color quenching. After neutralizing the mixture with 5 N HCl, 10 ml of scintillation cocktail (Scinti-A® XF : PPO/POPOP cocktail = 1 : 1) was added.

Analysis of total radioactivity

Total radioactivity in the biological samples was determined with a liquid scintillation counter (Rack Beta, LKB-Wallac Co.) after appropriate equilibration in darkness at 25°C. Total radioactivity was calculated in terms of dpm using the standard channel ratio quenching correction method. It should be noted that in the present study, the total radioactivity was measured and therefore represents not only [^{3}H]MTX but also the sum of all the radioactivity of [^{3}H]MTX, [^{3}H]MTX-HSA conjugates, HAMs containing [^{3}H]MTX and/or [^{3}H]MTX-HSA conjugates, and their metabolites.

Analysis of data

The area under the total radioactivity-time curves (AUC) and area under the total amounts of radioactivity-time curves from time zero to time infinity (AUQ, the product of AUC multiplied by the weight of tissue) were estimated by the trapezoidal rule-extrapolation method (Chiou, 1978; Chen et al., 1982). Standard methods (Gibaldi and Perrier, 1982) were used to calculate the following parameters based on plasma data for the small HAMs; the time-averaged total body clearance (CL), area under the first moment of plasma concentration-time curve (AUMC), mean residence time (MRT) and volume of distribution at steady state (V_{ss}). The mean values of apparent terminal half-life ($t_{1/2}$), V_{ss} and CL were determined by the harmonic mean method (Chiou, 1979).

Three indices for the evaluation of drug delivery into the targeting site were calculated based on AUQ as described by Gupta and Hung (1989): the weighted-average relative tissue exposure (r_e^*), weighted-average drug targeting efficiency against a given non-target tissue (t_e^*) and weighted-average composite or overall drug targeting efficiency (T_e^*).

$$(r_e^*)_i = (\mathrm{AUQ}_j)_{\mathrm{II\text{-}X}}/(\mathrm{AUQ}_i)_{\mathrm{I}} \quad (1)$$

$$t_e^* = \mathrm{AUQ}_{\mathrm{liver\ or\ lung}}/\mathrm{AUQ}_j \quad (2)$$

$$(T_e^*)_i = (\mathrm{AUQ}_i)/\sum \mathrm{AUQ} \quad (3)$$

where i denotes each tissue, I–X refer to treatments I–X, respectively, and j represents any tissue except the target tissue, the liver (for treatments III–VI) or the lung (for treatments VII–X). In this study, total radioactivity was measured only in the liver, lung, kidney and spleen, since

more than 90% of the total radioactivity administered was mainly distributed in these tissues.

Statistical analysis

The data were analyzed for statistical significance ($p < 0.05$) by analysis of variance (ANOVA) tests between means for unpaired data. All results are expressed as means for unpaired data. All results are expressed as mean ± standard deviation (S.D.).

Results and Discussion

The total radioactivities (as expressed in terms of [^{3}H]MTX) entrapped in the small and large HAMs are summarized in Table 1. In general, entrapment of total radioactivity increased with increasing ratios of [^{3}H]MTX-HSA conjugates to [^{3}H]MTX; the value increased 125, 93.9 and 62.6% for SHAMC, SHAMC3F, and SHAMCF, respectively, when compared with that of HAM containing only [^{3}H]MTX and the corresponding values for LHAMC, LHAMC3F, and LHAMCF were 79.8, 59.6 and 40.4%. The loading efficiencies (% of radioactivity entrapped in the HAMs when compared to the total radioactivity added during the preparation of the HAMs) were 95.6, 81.9, 68.8 and 42.3% for SHAMC, SHAMC3F, SHAMCF and SHAMF, respectively, and the corresponding values were 98.1, 86.9, 76.3 and 54.5% for LHAMC, LHAMC3F, LHAMCF and LHAMF. This might be due mainly to the fact that the [^{3}H]MTX in [^{3}H]MTX-HSA conjugate-

TABLE 1

Total radioactivity (as expressed in terms of [^{3}H]MTX) entrapped in the small and large HAMs

HAMs	Entrapped [^{3}H]MTX (nCi per mg microspheres)	Entrapped MTX [a] (μg per mg microspheres)
Small HAMs		
SHAMC	153	38.1
SHAMC3F	131	32.8
SHAMCF	110	27.5
SHAMF	67.7	16.9
Large HAMs		
LHAMC	157	39.2
LHAMC3F	139	34.8
LHAMCF	122	30.6
LHAMF	87.2	21.8

[a] Radioactivity of 4 nCi is equivalent to 1 μg of methotrexate.

TABLE 2

Particle size on a number and volume basis of the small and large HAMs

HAMs	Volume basis			Number basis		
	Mean diameter (μm)	$D_{90\%}$–$D_{10\%}$	SPAN	Mean diameter (μm)	$D_{90\%}$–$D_{10\%}$	SPAN
Small HAMs						
SHAMC	10.1	25.0	2.48	3.16	4.04	1.28
SHAMC3F	11.2	15.0	1.34	3.32	6.22	1.87
SHAMCF	8.35	10.9	1.31	3.38	5.19	1.54
SHAMF	10.4	8.30	0.798	3.53	8.19	2.32
Mean	10.0	14.8	1.48	3.35	5.91	1.75
±SD [a]	±1.04	±6.43	±0.615	±0.133	±1.53	±0.389
Large HAMs						
LHAMC	28.0	32.0	1.14	5.10	12.3	2.43
LHAMC3F	30.6	44.4	1.45	4.39	7.63	1.74
LHAMCF	18.0	20.4	1.13	5.12	10.3	2.01
LHAMF	13.0	14.2	1.09	3.44	8.19	2.38
Mean	22.4	27.8	1.20	4.51	9.61	2.14
±SD	±7.18	±11.5	±0.144	±0.69	±1.85	±0.282

[a] Standard deviation.

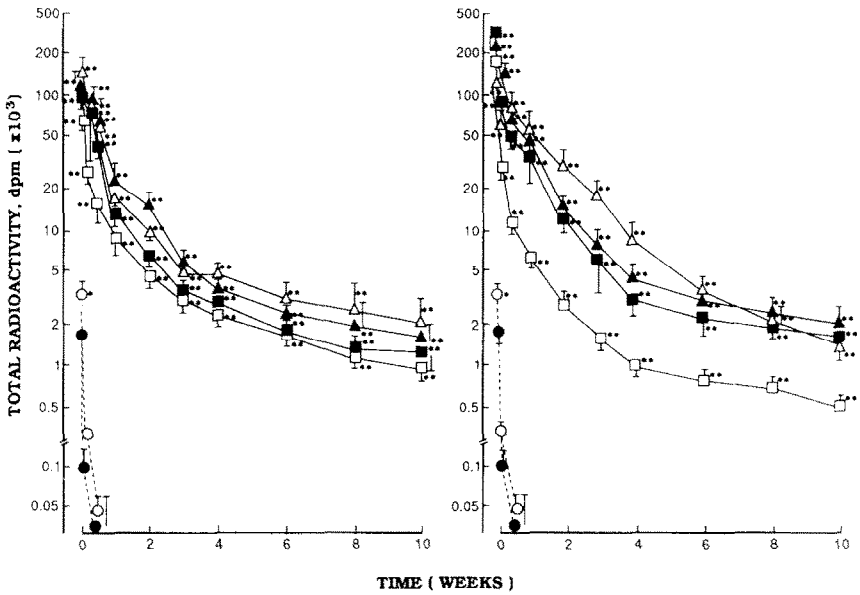

Fig. 1. Mean total radioactivity-time curves in the lung from treatments I (●), II (○), III (▲), IV (△), V (■) and VI (□) (left panel), and I (●), II (○), VII (▲), VIII (△), IX (■) and X (□) (right panel). Bars represent standard deviation. * $p < 0.05$, ** $p < 0.01$ when compared with the values from treatment I.

entrapped HAMs is covalently attached in the albumin matrix, however, the [^{3}H]MTX in [^{3}H]-MTX-entrapped HAMs is physically associated in the albumin matrix (Kim and Oh, 1988). MTX is known to bind physically to an extent of about 46% at normal clinical drug levels (Paxton, 1981).

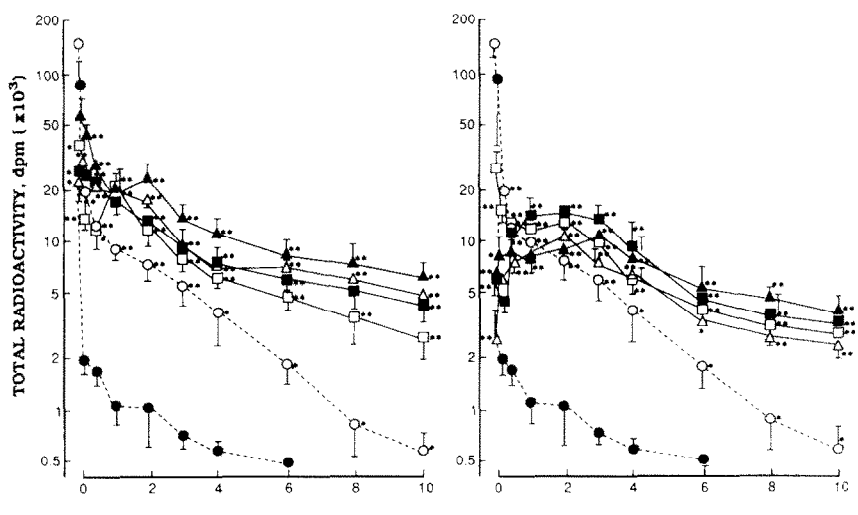

Fig. 2. Mean total radioactivity-time curves in the liver from treatments I (●), II (○), III (▲), IV (△), V (■) and VI (□) (left panel), and I (●), II (○), VII (▲), VIII (△), IX (■) and X (□) (right panel). Bars represent standard deviation. * $p < 0.05$, ** $p < 0.01$ when compared with the values from treatment I.

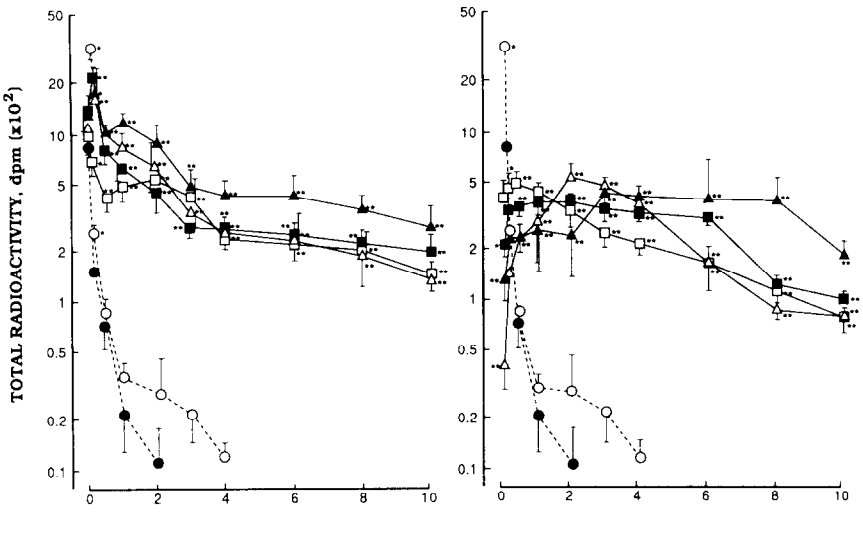

Fig. 3. Mean total radioactivity-time curves in the spleen from treatments I (●), II (○), III (▲), IV (△), V (■) and VI (□) (left panel), and I (●), II (○), VII (▲), VIII (△), IX (■) and X (□) (right panel). Bars represent standard deviation. * $p < 0.05$, ** $p < 0.01$ when compared with the values from treatment I.

Modification of the physicochemical characteristics of [^{3}H]MTX in [^{3}H]MTX-HSA conjugates such as the solubility, partitioning of drug into the oil or washing media during the preparation of the HAMs could also contribute to the increased entrapment of [^{3}H]MTX-HSA conjugates in HAMs (Sheu et al., 1986). The loss of entrapped [^{3}H]MTX-HSA conjugates from the

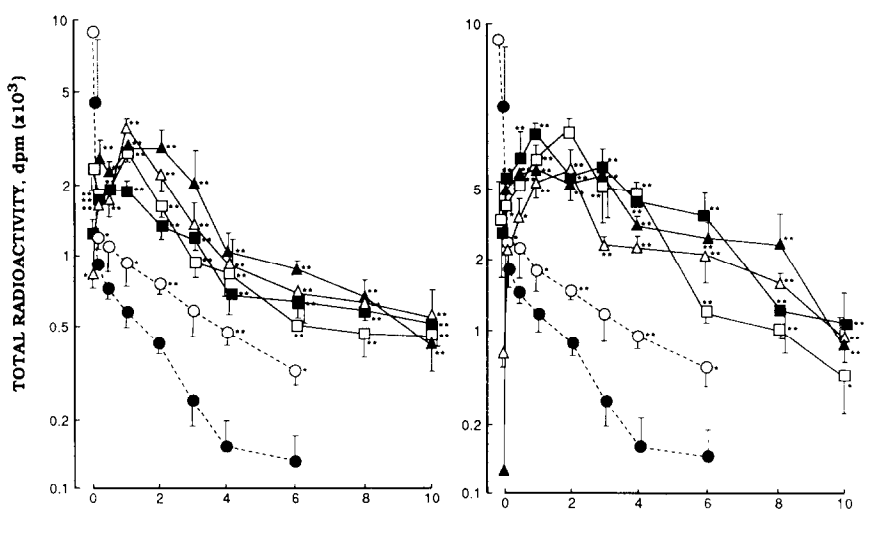

Fig. 4. Mean total radioactivity-time curves in the kidney from treatments I (●), II (○), III (▲), IV (△), V (■) and VI (□) (left panel), and I (●), II (○), VII (▲), VIII (△), IX (■) and X (□) (right panel). Bars represent standard deviation. * $p < 0.05$, ** $p < 0.01$ when compared with the values from treatment I.

core of the HAMs could be reduced due to the relatively large size of the conjugate when compared to that of free [^{3}H]MTX during the preparation of the HAMs. It should be noted that the total amounts of albumin were almost equal in the small and large HAMs, respectively, when considering the amounts of entrapped MTX per mg microsphere (Table 1).

The mean diameters on a volume and number basis of the HAMs are summarized in Table 2. The mean diameters were significantly greater in the large HAMs than those of the small HAMs; the values on a volume and number basis were 10.0 ± 1.04 and 3.35 ± 0.133 μm, respectively, for the small HAMs, and the corresponding values for the large HAMs were 22.4 ± 7.18 and 4.51 ± 0.69 μm. However, the SPAN values were not significantly different between the small and large HAMs.

The mean total radioactivity-time profiles in the lung, liver, spleen, and kidney are shown in Figs 1–4, respectively, from treatments I–X, and the corresponding mean values of AUQ, r_c^*, t_c^* and T_c^* for the organs studied are listed in Tables 3–6, respectively. The total radioactivity was always greater from treatment II than that from treatment I in all the organs studied and might be due to extensive entrapment of [^{3}H]MTX-HSA conjugates in the organs and slow release of [^{3}H]MTX from the conjugates. Some MTX-RSA conjugates appeared to be taken up into the tissues and MTX was released slowly from the conjugates when the conjugates were infused intravenously to rabbits (Yoon et al., 1991). The considerable uptake of MTX-HSA conjugates in the liver could be expected in view of the report that macromolecular prodrugs, e.g., mitomycin C-dextran conjugate accumulated predominantly in the reticuloendothelial organs such as the liver and spleen when administered systemically (Takamura et al., 1986). However, the total radioactivity from treatments III–X (Figs 1–4) was always lower for up to 2 days after an i.v. administration than those from treatments I and II, and higher thereafter in the all organs studied except in the lung (Fig. 1). For example, the total radioactivity in the lung increased immediately in a few minutes after i.v. injection, then declined rapidly up to 3–4 weeks and declined slowly thereafter from treatments III–X. During the

TABLE 3

Area under the mean total amount of radioactivity vs time curve (AUQ) from treatments I–X

Treatment	AUQ ($\times 10^3$ dpm day)					
	Lung	Liver	Spleen	Kidney	Plasma	Sum
I	0.590	56.5	0.824	18.3	7.14	83.3
II	0.779	360	2.27	41.0	12.5	417
Small HAMs						
III	795	1 300	68.8	109	15.3	2 290
IV	759	1 010	45.0	103	12.8	1 930
V	518	892	35.2	90.8	11.3	1 550
VI	332	699	30.3	85.8	8.27	1 160
Mean	601	976	44.8	97.2	11.9	1 730
±SD [a]	±188	±218	±14.8	±9.26	±2.55	±423
Large HAMs						
VII	1 170	583	30.6	125		1 910
VIII	1 140	507	19.2	108		1 780
IX	834	574	22.8	126		1 560
X	254	544	17.9	107		924
Mean	851	552	22.6	116		1 540
±SD	±369	±29.7	±4.93	±8.95		±379

[a] Standard deviation.

rapid decrease in radioactivity in the lung, the radioactivity in the liver, spleen and kidney generally increased slowly (Figs 2–4). This might be due to the rapid uptake of the HAMs by the lung through mechanical filtration just after i.v. administration owing to their large size and slow redistribution into the liver, spleen and kidney due to either the HAMs being degraded sufficiently for the size to allow passage through the capillary beds of the lung and/or the release of [^{3}H]MTX or [^{3}H]MTX-HSA conjugate from the HAMs.

The values of AUQ were higher in the lung, liver, spleen and kidney from treatments III–X than those from treatments I and II, and were higher from treatment II than treatment I (Table 3). This might be due to the increased entrapment of HAMs and/or [^{3}H]MTX-HSA conjugates in the lung, liver, spleen and kidney, and slow release of [^{3}H]MTX and/or [^{3}H]MTX-HSA conjugates from the HAMs from treatments II–X. The release of MTX from MTX-BSA (Halbert et al., 1987), MTX-HSA (Kim et al., 1989b) and MTX-RSA (Yoon et al., 1991) was slow when the conjugates were incubated in various solutions. The release of MTX (the concentrations of MTX were measured spectrophotometrically) from the large HAMs decreased with increasing ratios of MTX-HSA conjugates to free MTX using a dissolution tester containing 0.5 M phosphate-buffered saline solution of pH 7.4 kept at 37°C and at a rate of 100 rpm (data not shown). It is of interest to note that the highest value of AUQ was ob-

TABLE 4

Weighted-average relative tissue exposure (r_e^*) to treatment I (or II) from treatments II (or III)–X

Treatment	Lung	Liver	Spleen	Kidney	Plasma	Sum
II	1.32	6.38	2.75	2.24	1.75	5.00
Small HAMs						
III	1350 [a]	23.0	83.5	5.95	2.15	27.5
	(1020) [b]	(3.61)	(30.4)	(2.66)	(1.23)	(5.50)
IV	1290	17.9	54.6	5.66	1.79	23.2
	(977)	(2.81)	(19.9)	(2.53)	(1.02)	(4.64)
V	878	15.8	42.7	4.97	1.58	18.6
	(665)	(2.48)	(15.5)	(2.22)	(0.903)	(3.72)
VI	563	12.4	36.8	4.69	1.16	13.9
	(427)	(1.95)	(13.4)	(2.09)	(0.663)	(2.78)
Mean	1020	17.3	54.4	5.32	1.67	20.8
±SD [c]	±319	±3.86	±18.0	±0.507	±0.358	±5.08
	(772)	(2.71)	(19.8)	(2.38)	(0.954)	(4.16)
	(±242)	(±0.602)	(±6.55)	(±0.229)	(±0.205)	(±1.02)
Large HAMs						
VII	1990	10.3	37.1	6.82	–	22.9
	(1510)	(1.62)	(13.5)	(3.04)		(4.58)
VIII	1940	8.98	23.3	5.89	–	21.4
	(1470)	(1.41)	(8.47)	(2.63)		(4.28)
IX	1410	10.2	27.6	6.89	–	18.7
	(1070)	(1.60)	(10.0)	(3.08)		(3.74)
X	431	9.64	21.8	5.86	–	11.1
	(327)	(1.51)	(7.93)	(2.62)		(2.22)
Mean	1440	9.78	27.5	6.37	–	18.5
±SD	+626	±0.526	±5.99	±0.490		±4.55
	(1084)	(1.53)	(9.88)	(2.84)	–	(3.71)
	(±476)	(±0.0832)	(±2.27)	(±0.218)		(±0.909)

[a] Based on treatment I [$(AUQ_i)_{II-X}/(AUQ_i)_I$].
[b] Based on treatment II [$(AUQ_i)_{III-X}/(AUQ_i)_{II}$].
[c] Standard deviation.

TABLE 5

Weighted-average targeting efficiency for liver (treatments III–VI) and lung (treatments VII–X) against a given non-target tissue (t_e^*) from treatments I–X

Treatment	Lung	Liver	Spleen	Kidney
I	95.7	0.0104	0.716	0.0322
II	462	0.00216	0.343	0.0190
Small HAMs				
III	1.64	–	18.9	12.0
IV	1.33	–	22.5	9.77
V	1.72	–	25.4	9.82
VI	2.10	–	23.0	8.15
Mean	1.70	–	22.4	9.93
±SD [a]	±0.275		±2.31	±1.35
Large HAMs				
VII	–	2.01	38.3	9.40
VIII	–	2.26	59.7	10.6
IX	–	1.45	36.7	6.63
X	–	0.47	14.2	2.37
Mean	–	1.55	37.2	7.26
±SD		±0.688	±16.1	±3.17

[a] Standard deviation.

TABLE 6

Weighted-average overall targeting efficiency (T_e^*) from treatments I–X

Treatment	Lung	Liver	Spleen	Kidney	Plasma
I	0.708	67.8	0.989	21.9	8.57
II	0.187	86.4	0.545	9.85	2.30
Small HAMs					
III	34.7	56.8	3.00	4.76	0.668
IV	39.3	52.3	2.33	5.34	0.663
V	33.4	57.5	2.27	5.86	0.729
VI	28.6	60.3	2.61	7.40	0.713
Mean	34.0	56.7	2.55	5.84	0.693
±SD [a]	±3.81	±2.87	±0.288	±0.981	±0.0284
Large HAMs					
VII	61.3	30.5	1.60	6.53	–
VIII	64.4	28.5	1.08	6.05	–
IX	53.6	36.9	1.46	8.08	–
X	27.5	58.9	1.94	11.6	–
Mean	51.7	38.7	1.52	8.07	–
±SD	±14.5	±12.1	±0.308	±2.18	

[a] Standard deviation.

tained for the liver after i.v. administration of small HAMs (treatments III–VI) and [^{3}H]MTX-HSA conjugates (treatment II), and for the lung after large HAMs (treatments VII–X). It suggested that the small (including [^{3}H]MTX-HSA conjugates) and large HAMs could have a better targeting ability to the liver and lung, respectively, than that of free MTX or MTX-HSA conjugates. This appears to be supported by the higher value of r_e^* for the liver and lung from small (including [^{3}H]MTX-HSA conjugates) and large HAMs, respectively (Table 4). The data in parentheses which are listed in Table 4 represent the r_e^* values on comparing the values from treatment II: the higher values of r_e^* for the liver and lung indicate that the small and large HAMs have a better targeting efficiency to the liver and lung than that of [^{3}H]MTX-HSA conjugates. Table 5 lists the t_e^* values when the liver and lung were chosen as a targeting organ for the small and large HAMs, respectively, since the highest values of AUQ for the liver and lung were obtained from the small and large HAMs, respectively (Table 3). Values of t_e^* greater than unity in Table 5 indicate that small and large HAMs have a greater selectivity for the liver and lung, respectively, than other organs. The T_e^*

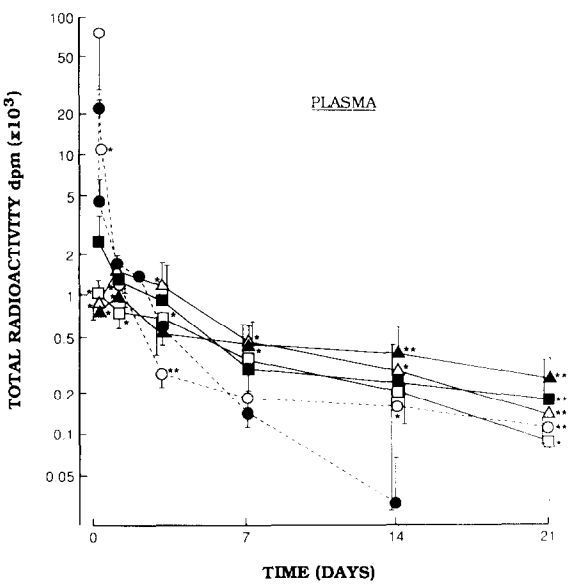

Fig. 5. Mean plasma total radioactivity-time curves from treatments I (●), II (○), III (▲), IV (△), V (■) and VI (□). Bars represent standard deviation. * $p < 0.05$, ** $p < 0.01$ when compared with the values from treatment I.

TABLE 7

Mean pharmacokinetic parameters of plasma total radioactivity after i.v. administration of [^{3}H]MTX (treatment I), [^{3}H]MTX-HSA conjugates (treatment II), SHAMC (treatment III), SHAMC3F (treatment IV), SHAMCF (treatment V) and SHAMF (treatment VI) to mice (n = 4)

	Treatment					
	I	II	III	IV	V	VI
AUC (dpm day ml^{-1})	4580	7950	11100	8380	9570	5340
AUMC (dpm day^2 ml^{-1})	12200	79400	294000	87700	218000	51300
MRT (day)	2.66	10.0	26.5	10.1	22.8	9.61
CL (ml day^{-1})	72.7	41.9	30.1	39.7	34.8	62.4
V_{ss} (ml)	193	419	799	416	794	599
$t_{1/2}$ (day)	2.70	13.8	19.4	8.66	20.2	6.83

1 nCi = 2.22×10^6 dpm.

values are listed in Table 6. The small and large HAMs show the highest T_e* value for the liver and lung, respectively, indicating that the small and large HAMs have better targeting efficiencies to the liver and lung than those from treatments I and II. However, the liver targeting efficiency from treatment II appeared to be similar to those from small HAMs. The results are consistent with the report that "intravenous delivery of particles above 7–12 μm leads to their mechanical filtration by the lungs, whereas particles between 3 and 12 μm will become entrapped within the capillary networks of the lung, liver and spleen" (Burger et al., 1985).

The mean total radioactivity-time profiles in plasma from treatments I–IV are shown in Fig. 5, and the corresponding pharmacokinetic parameters are listed in Table 7. The total radioactivity declined polyexponentially with increased terminal half-life from treatments II–X compared with from treatment I. It resulted in increased AUC and decreased CL from treatments II–VI (Table 7). MTX is excreted via the kidney, the main elimination organ for MTX in humans (Shen and Azarnoff, 1978), dogs (Lui et al., 1985) and rabbits (Chen and Chiou, 1983), however, [^{3}H]MTX-HSA conjugates and the HAMs themselves could not be excreted via the kidney. Therefore, the almost constant total plasma radioactivity from 7 to 21 days from treatments II–VI might be due mainly to slow release of [^{3}H]MTX from [^{3}H]-MTX-HSA conjugates (treatment II) or slow release of [^{3}H]MTX and/or [^{3}H]MTX-HSA conjugates from the HAMs (treatments III–VI) which were taken up into tissues such as lung (Fig. 1), liver (Fig. 2), spleen (Fig. 3) and kidney (Fig. 4) and/or presented in plasma. Evidence in support of this contention is provided by the increased values of V_{ss} and MRT from treatments II–IV (Table 7). It should be noted that the radioactivity in plasma was measured only up to 21 days and might be due to our assay sensitivity. Although the radioactivity in plasma was not determined from the large HAMs, the patterns of radioactivity-time curves in plasma from the large HAMs might be similar to those from the small HAMs, since the patterns of radioactivity-time curves in the lung, liver, spleen and kidney were similar between the small and large HAMs (Figs 1–4).

If the present study on mice could be extrapolated to humans, in vivo drug release can be controlled rationally at the desired rate by varying the ratios of MTX-HSA conjugates to MTX during the preparation of HAMs, and organ targeting can be controlled by adjusting the size distribution of the microspheres.

Acknowledgement

This work was supported in part by a research grant from the Korea Science and Engineering Foundation (KOSEF 860-414) in 1986–1989.

References

Burger, J.J., Tomlinson, E., Mulder, E.M.A. and McVie, J.G., Albumin microspheres for intra-arterial tumour targeting.

I. Pharmaceutical aspects. *Int. J. Pharm.*, 23 (1985) 333–344.

Bushi, H., Fujiwara, E. and Ferszt, D.C., Studies on the metabolism of radioactive albumin in tumor-bearing rats. *Cancer Res.*, 21 (1961) 371–377.

Cerrottini, J.C. and Isliker, H., Transport of cytostatic agents by plasma proteins I. Penetration of serum albumin into tumor cells. *Eur. J. Cancer*, 3 (1967) 111–124.

Chen, M.L., Lam, G., Lee, M.G. and Chiou, W.L., Arterial and venous blood sampling in pharmacokinetics: Griseofulvin. *J. Pharm. Sci.*, 71 (1982) 1386–1389.

Chen, M.-L. and Chiou, W.L., Pharmacokinetics of methotrexate and 7-hydroxymethotrexate in rabbits after intravenous administration. *J. Pharmacokinet. Biopharm.*, 11 (1983) 1–13.

Chiou, W.L., Critical evaluation of potential error in pharmacokinetic studies using the linear trapezoidal rule method for the calculation of the area under the plasma level-time curve. *J. Pharmcokinet. Biopharm.*, 6 (1978) 539–546.

Chiou, W.L., New calculation method for mean apparent drug volume of distribution and application to rationale dosage regimen. *J. Pharm. Sci.*, 68 (1979) 1067–1069.

Chu, B.C.F. and Whiteley, J.M., High molecular weight derivatives of methotrexate as chemotherapeutic agents. *Mol. Pharmacol.*, 13 (1977) 80–88.

Chu, B.C.F. and Whiteley, J.M., Control of solid tumor metastases with a high-molecular-weight derivatives of methotrexate. *J. Natl. Cancer Inst.*, 62 (1979) 79–81.

Gibaldi, M. and Perrier, D., *Pharmacokinetics*, 2nd Edn, Dekker, New York, 1982.

Gupta, P.K. and Hung, C.T., Quantitative evaluation of targeted drug delivery systems. *Int. J. Pharm.*, 56 (1989) 217–226.

Halbert, G.W., Florence, A.T. and Stuart, J.F.B., Characterization of in-vitro drug release and biological activity of methotrexate-bovine serum albumin conjugates. *J. Pharm. Pharmacol.*, 39 (1987) 871–876.

Jacobs, S.A., D'Urso-Scott, M. and Bertino, J.R., Some biochemical and pharmacologic properties of amethopterin-albumin. *Ann. N.Y. Acad. Sci.*, 186 (1971) 284–286.

Jusko, W.J. and Gretch, M., Plasma and tissue protein binding of drugs in pharmacokinetics. *Drug. Metab. Res.*, 5 (1976) 43–140.

Kim, C.-K. and Park, D.K., Stability and drug release properties of liposomes containing cytarabine as a drug carrier. *Arch. Pharm. Res.*, 10 (1987) 75–79.

Kim, C.-K. and Oh, Y.-K., Development of hydrophilic human serum albumin microspheres using a drug-albumin conjugates. *Int. J. Pharm.*, 47 (1988) 163–169.

Kim, C.-K., Kwon, K.A., Jeong, E.J. and Lee, M.G., Effects of molecular weights on the physico-pharmaceutical properties of poly-L-glutamic acid-cytarabine conjugates. *Arch. Pharm. Res.*, 12 (1989a) 88–93.

Kim, C.-K., Lee, M.G., Park, M.K., Lee, H.-J. and Kang, H.J., In vitro drug release characteristics of methotrexate-human serum albumin conjugates. *Arch. Pharm. Res.*, 12 (1989b) 186–190.

Kramer, P.A., Albumin microspheres as vehicles for achieving specificity in drug delivery. *J. Pharm. Sci.*, 63 (1976) 1646–1647.

Lee, M.G., Lui, C.Y., Chen, M.L. and Chiou, W.L., Pharmacokinetics of drug in blood IV: Unusual distribution, storage effect and metabolism of methotrexate. *Int. J. Clin. Pharmacol. Ther. Toxicol.*, 22 (1984) 530–537.

Lee, M.G., Lui, C.Y. and Chiou, W.L., Pharmacokinetics of drug in blood V: Aberrant blood and plasma concentration profiles of methotrexate during intravenous infusion. *Biopharm. Drug Disp.*, 7 (1986) 487–494.

Longo, W.E. and Goldberg, E.P., Hydrophilic albumin microsphere. *Methods Enzymol.*, 112 (1985) 18–26.

Lui, C.Y., Lee, M.G. and Chiou, W.L., Clearance studies of methotrexate in dogs after multiple-rate infusion. *Cancer Res.*, 45 (1985) 1545–1548.

Paxton, J.W., Protein binding of methotrexate in sera from normal human being: Effect of drug concentration, pH, temperature and storage. *J. Pharmacol. Methods*, 5 (1981) 203–213.

Ryser, H.J.-P., The measurement of ^{131}I-serum albumin uptake by tumor cells in tissue culture. *Lab. Invest.*, 12 (1963) 1009–1017.

Shen, D.D. and Azarnoff, D.L., Clinical pharmacokinetics of methotrexate. *Clin Pharmacokinet.*, 3 (1978) 1–13.

Sheu, M.T., Moustafa, M.A. and Sokoloski, T.D., Entrapment of bioactive compounds within native albumin beads. II. Effects of rate and extent of cross-linking on microbeads properties. *J. Parent. Sci. Technol.*, 40 (1986) 253–258.

Takamura, Y., Mori, K., Hashida, M. and Sezaki, H., Absorption characteristics of macromolecular prodrug of mitomycin C following intramuscular administration. *Chem. Pharm. Bull.*, 34 (1986) 1775–1783.

Torrado, J.J., Illum, L. and Davis, S.S., Particle size and size distribution of albumin microspheres produced by heat and chemical stabilization. *Int. J. Pharm.*, 51 (1989) 85–90.

Willmot, N., Chen, Y., Goldberg, J., Mcardle, C. and Florence, A.T., Biodegradation rate of embolized protein microspheres in lung, liver and kidney of rats. *J. Pharm. Pharmacol.*, 41 (1989) 433–438.

Yang, J.-S., Development of liver-targeting adriamycin delivery system using human serum albumin microspheres. Ph.D Thesis, Seoul National University, Seoul, Korea, 1986.

Yoon, E.J., Chang, H.W., Lee, M.G., Lee, H.-J., Park, M.K. and Kim, C.-K., Pharmacokinetics of methotrexate after intravenous infusion of methotrexate-rabbit serum albumin conjugate to rabbits. *Int. J. Pharm.*, 67 (1991) 177–184.